6) More complicated configurations. The present vortex method has been extended to more complicated configurations. One of them involves as many as four missile-launchers on a vertical pylon (two on each side of the pylon), and the other has two vertical pylon-missile combinations on each side of the airplane.

References

[1] Spreiter, J. R., "The Aerodynamic Forces on Slender Plane- and Cruciform-Wing and Body Combinations," TR 962, 1950, NACA.

[2] Spreiter, J. R., "On Slender Wing-Body Theory," *Journal of the Aeronautical Sciences*, Vol. 19, No. 8, Aug. 1952, pp. 571–572.

[3] Ward, G. N., "Supersonic Flow past Slender Pointed Bodies," *Quarterly Journal of Mechanics and Applied Mathematics*, Vol. 2, Pt. 1, 1949, pp. 75–97.

[4] Adams, M. C. and Sears, W. R., "Slender-Body Theory–Review and Extension," *Journal of the Aeronautical Sciences*, Vol. 20, No. 2, Feb. 1953, pp. 85–98.

[5] Nielsen, J. N., *Missile Aerodynamics*, 1st ed., McGraw-Hill, New York, 1960, pp. 131–140, pp. 156–165.

[6] Campbell, G. S., "A Finite Vortex Method for Slender Wing-Body Combinations," *Journal of the Aeronautical Sciences*, Vol. 25, No. 1, Jan. 1958, pp. 60–61.

[7] Campbell, G. S., "Characteristics of Slender Wing-Body Combinations with Folding Wings," *Aircraft Engineering*, Jan. 1959, pp. 1–8.

[8] Yang, H. T., "Remarks on the Vortex Model of Wing-Body Interference," *AIAA Journal*, Vol. 5, No. 3, March 1967, p. 607.

[9] Milne-Thomson, L. M., *Theoretical Hydrodynamics*, 5th ed., Macmillan, New York, 1968, p. 157, p. 364.

[10] Glauert, H., *The Elements of Airfoil and Airscrew Theory*, 2nd ed., Cambridge University Press, New York, 1947, p. 55.

[11] Lawrence, H. R., "The Lift Distribution on Low Aspect Ratio Wings at Subsonic Speeds," *Journal of the Aeronautical Sciences*, Vol. 18, No. 10, Oct. 1951, p. 638–695.

[12] Lomax, H. and Sluder, L., "Chordwise and Compressibility Corrections to Slender Wing Theory," TR 1105, 1952, NACA.

[13] Sacks, A. H., Lundberg, R. E., and Hanson, C. W., "A Theoretical Investigation of the Aerodynamics of Slender Wing-Body Combinations Exhibiting Leading-Edge Separation," CR-719, March 1967, NASA.

[14] Sacks, A. H., "Aerodynamic Forces, Moments, and Stability Derivatives for Slender Bodies of General Cross Section," TN 3283, Nov. 1954, NACA.

[15] Skulsky, R. S., "A Conformal Mapping Method to Predict Low-Speed Aerodynamic Characteristics of Arbitrary Slender Re-Entry Shapes," *Journal of Spacecraft and Rockets*, Vol. 3, No. 2, Feb. 1966, pp. 247–253.

NOV.-DEC. 1968 J. AIRCRAFT VOL. 5, NO. 6

Review of Methods for Predicting the Aerodynamic Characteristics of Parawings

MICHAEL R. MENDENHALL,* SELDEN B. SPANGLER,† AND JACK N. NIELSEN‡

Nielsen Engineering & Research Inc., Palo Alto, Calif.

A review is made of methods for predicting the aerodynamic characteristics of one- and two-lobed conical parawings and all-flexible parawings, with emphasis on the low-speed characteristics of conical two-lobed parawings. Methods are reviewed and compared for predicting canopy shape and parawing lift, drag, and pitching moment. A discussion is given of the effects of leading-edge booms on the aerodynamic characteristics. Comparison is made between experiment and prediction for flexible parawings and rigid wings of parawing shape.

Nomenclature

A = aspect ratio, b^2/S
b = span of wing
c = local chord
c_d = section drag coefficient, based on local chord
c_l = section lift coefficient, based on local chord
$c_{l\alpha}$ = section lift-curve slope, per rad
$c_{l_{max}}$ = maximum section lift coefficient
c_r = root chord
C_D = wing drag coefficient, based on planform area S
C_{Di} = wing-induced drag coefficient, based on planform area S
C_L = wing lift coefficient, based on planform area S
$C_{L\alpha}$ = wing lift-curve slope, $dC_L/d\alpha$, per rad
C_m = wing pitching-moment coefficient, based on planform area S, and mean aerodynamic chord
C_{m_α} = wing moment-curve slope, $dC_m/d\alpha$, per rad
C_{m_0} = wing pitching-moment coefficient at zero wing lift
d = diameter of leading-edge boom
f = maximum ordinate of camber section
l = projected trailing-edge length of inflated parawing measured in planform
l_0 = value of l for uninflated planform
l' = canopy trailing-edge length of inflated triangular parawing
q = freestream dynamic pressure
s = semispan
S = wing planform area, inflated
T = spanwise tension per unit chord
x, y, z = wing axes, Fig. 1
α = angle of attack
α_0 = angle of attack for zero lift
α_l = luffing angle of attack
ϵ = semiapex angle of inflated planform
λ = tension parameter, Eq. (1)
Λ = sweep angle of leading edge of inflated planform
β = half of angle subtended at cone axis by a parawing lobe lying on the surface of a circular cone; a half-cone corresponds to $\beta = 90°$
$\Delta\Lambda$ = difference in sweep angle of leading edge between inflated and uninflated states

Subscripts

M = value given by Multhopp method
W = value given by Weissinger method

Presented as Paper 68-10 at the AIAA 6th Aerospace Sciences Meeting, New York, January 22–24, 1968; submitted January 11, 1968; revision received June 20, 1968.

* Research Engineer. Associate Member AIAA.

† Vice President. Fellow AIAA.

‡ President. Associate Fellow AIAA.

Introduction

MANY research and development programs have been conducted on parawings (flexible wings) since Rogallo's pioneering paper in 1954.[1] This work was prompted by the capability of the parawing to provide reasonable glide capability with a lifting surface that could be collapsed to minimize storage volume. Early applications involved conical parawings with large, inflated leading edges, such as the Gemini parawing.[2] Later applications involved parawings with small leading edges, such as the Army Precision Drop Glider.[3] More recently, there has been considerable interest in all-flexible parawings, which have no rigid members and can be treated like parachutes for stowage and deployment purposes.

Because of inherent difficulties in the theoretical treatment of flexible, aerodynamic lifting surfaces, most of the work to date on parawings has been experimental in nature, and has been directed toward providing empirical information for design purposes and for developing specific vehicles. Much of this work has been conducted at the NASA Langley Research Center. The theory of flexible air-foils at low speeds was independently developed in three different countries by three different investigators.[4–6] Subsequently, Nielsen et al.[7–12] and Gersten and Hucho[13] applied slender-body methods to the development of theories for the low-speed aerodynamic performance of low-aspect-ratio, low-slackness conical parawings. References 7–11 represent work sponsored by Air Programs, Office of Naval Research, and Ref. 12 represents work sponsored by the Army Research Office, Durham, N.C. Recently, the present authors, under a NASA contract for Langley Research Center, used the Polhamus-Naeseth method[14] in a detailed investigation of conical two-lobed parawings, including consideration of drag. Most of the two-lobed conical parawing results reported herein are based on this investigation.

No theoretical studies of parawing aerodynamics are available for transonic or supersonic speeds. Fralich[15] has developed three-dimensional canopy stress shape relations, with which he used Newtonian theory to predict parawing performance at hypersonic speeds.

The purpose of this paper is to review the available analytical methods for predicting the aerodynamic characteristics of conical and all-flexible parawings. Methods are considered for determining canopy shape and wing aerodynamic characteristics. Comparisons with data are shown, where possible. Limitations of present methods are noted, and suggestions for new areas of research are made.

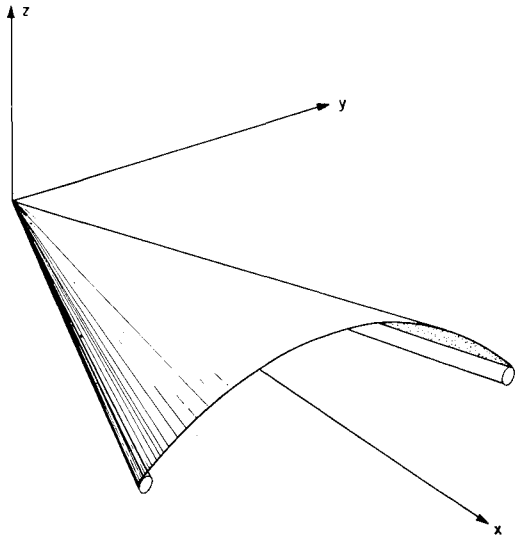

Fig. 1 One-lobed conical parawing.

General Properties of Parawings

Parawings can be classified into rigid-boom parawings and all-flexible parawings. Rigid-boom parawings have solid or inflated booms along the two swept leading edges of the planform. This type can be further divided into one-lobed parawings (Fig. 1) and two-lobed parawings that utilize a rigid keel. The diameter of the rigid members may be large, compared to the root chord, as in the inflatable-boom Gemini parawing, or small, as in the Army Precision Drop Glider. In the former case, the boom must be considered an integral part of the canopy for aerodynamic performance prediction, and no rational prediction methods exist. In the latter case, the effect of the boom on parawing performance is relatively small, and the boom may be considered to add incremental forces and moments to those of the basic canopy. The methods reviewed herein apply only to the small-boom case.

All-flexible parawings (Fig. 2) have no rigid members and must depend upon a number of suspension lines along the leading edges and keel(s) to control the canopy shape. No general prediction methods exist for all-flexible parawings.

A rigorous theory for the aerodynamic characteristics of a parawing requires a simultaneous solution for both shape and loading. This approach has proven possible for low-aspect-ratio conical parawings using slender-body theory. For high-aspect-ratio parawings, the most successful approach has been to assume a canopy shape, based on experimental observations, and then to apply rigid-wing theory to predict aerodynamic performance.

One-Lobed Conical Parawings

A theoretical method for the prediction of the shape and loading of one-lobed conical parawings has been developed on the basis of slender-body theory. The method includes both longitudinal and lateral motion, and is limited to the case of no leading-edge boom, low-aspect ratio, and relatively low slackness.

Longitudinal Characteristics

The slender-body solution for the one-lobed conical parawing is presented in Ref. 7. The basic differential equation is derived from a force balance in the crossflow plane between the pressure difference across the canopy, the spanwise tension, and the local curvature. A perturbation velocity potential is written for the potential flow in the crossflow plane. With the use of a boundary condition of zero flow through the canopy, the force balance equation can be solved to yield the canopy shape and perturbation velocity components in the form of Fourier series. From auxiliary relations, the surface pressures and the aerodynamic lift and drag coefficients can be determined.

In nondimensional form, the shapes, loadings, and other aerodynamic characteristics of a one-lobed parawing are func-

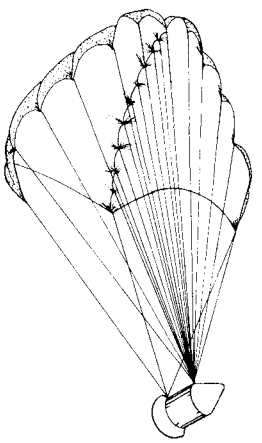

Fig. 2 All-flexible parawing.

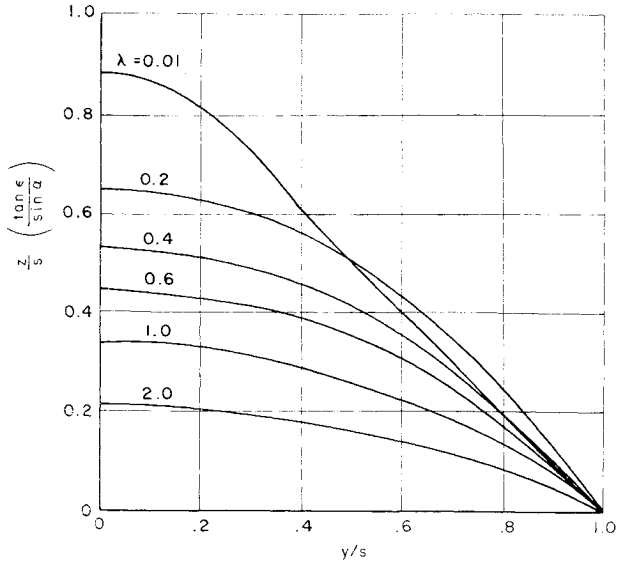

Fig. 3 Canopy sections for one-lobed conical parawing.

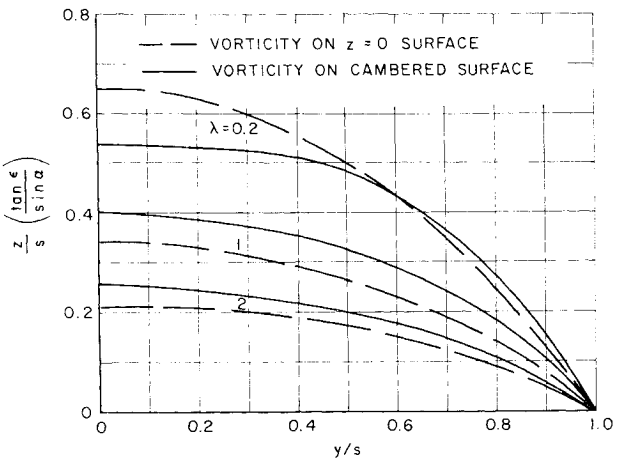

Fig. 4 Effect of location of bound vorticity on canopy shape of slender one-lobed parawing.

tions of only one variable, the tension parameter λ.

$$\lambda = T/4 \text{ sq } \tan^2\epsilon \qquad (1)$$

A series of tabulations is presented in Ref. 7 for various values of λ from 10^{-2} to 10^{2} which completely describes, in nondimensional form, the shapes and aerodynamic characteristics of all one-lobed, conical parawings.

Typical cross-section shapes are shown in Fig. 3. As λ decreases, the slackness for a given ϵ and α increases. When λ reaches a value of about 0.21, the leading-edge singularity disappears. This condition corresponds to the movement of the stagnation point from the lower surface of the wing to the leading edge, which is the condition for luffing of the canopy. A simple equation for the luffing angle of attack can be written in terms of slackness and ϵ. Theoretical results for the variation of lift and induced drag with slackness and semiapex angle are included in Ref. 7. The method does not include prediction of profile drag.

In the analysis of Ref. 7, the bound vorticity is placed in the plane of the leading edges ($z = 0$) and the boundary condition of no flow through the wing surface is also satisfied there. Gersten and Hucho,[13] in their slender-body analysis of one-lobed conical parawings, examined the effect of placing the bound vorticity on the canopy surface rather than in the plane of the leading edges. There is a significant effect on canopy shape for a given value of tension parameter, as shown in Fig. 4. However, for moderate to large values of the tension parameter, there is little difference in shape for the same slackness ratio.

Limited comparisons of the theory of Ref. 7 with data for aspect ratios 1, 2, and 3, and slackness ratios up to 0.04 given in Refs. 8 and 9, indicate that canopy shape, angle of zero lift, and luffing angle are well predicted. Lift-curve-slope comparisons indicate that the slender-body method becomes inaccurate for aspect ratios greater than 2. No drag or moment comparisons were made.

Lateral Characteristics

The one-lobed conical parawing is the only configuration for which a theory including sideslip has been developed. The theory, described in Ref. 12, is an extension of the theory of Ref. 7 to small, horizontal crossflow, assuming no circulation in the crossflow plane. The resulting nondimensional wing characteristics depend only on the tension parameter λ and the ratio of sideslip angle to wing semiapex angle. An extensive tabulation of wing characteristics is presented in Ref. 12. No comparison between theory and experiment is presented because of lack of suitable data.

Two-Lobed Conical Parawings

Much of the theoretical analysis of parawings has been devoted to two-lobed conical parawings, primarily because most parawing applications to date have employed this configuration. As indicated earlier, the theoretical analysis is limited to parawings with relatively small leading-edge booms, so that the boom force and moment increments can be added to those of the basic canopy to get over-all performance. The areas discussed are basic canopy prediction methods, comparison of these methods, and comparisons with experiment, which include leading-edge effects.

Basic-Canopy Prediction Methods

Two basic approaches to the prediction of canopy low-speed aerodynamic characteristics are slender-body theory, in which both shape and loading are obtained simultaneously, and lifting-surface theory, applied to an assumed canopy shape. These methods must be supplemented by a profile-drag prediction method.

Slender-body theory

On the basis of conical slender-body theory, the geometric and aerodynamic characteristics of two-lobed parawings were determined in Ref. 8 in a manner similar to that used for one-lobed parawings in Ref. 7. Since two-lobed parawings possess a cusp at the root chord in their cross-sectional shapes, special mathematical treatment beyond that used for one-lobed parawings is required.

As was found for the one-lobed parawing, it is possible to describe the aerodynamic characteristics nondimensionally as a function of the tension parameter λ. A systematic series of tables yielding the complete geometric and aerodynamic characteristics of all triangular two-lobed parawings is given in Ref. 8. These results are restricted to small angles of attack, low aspect ratios, and relatively low slackness.

The nondimensional cross-sectional shapes are a unique function of the tension parameter and are shown in Fig. 5. The maximum ordinate occurs slightly outboard of the midspan position for $\lambda > 0.2$. With decreasing λ (tension), the position of the maximum ordinate moves toward the root chord. For $\lambda < 0.2$, undulations, which are associated with a change in the sign of the leading-edge singularity, appear in the shape near the wing tip. It is interesting that the value of $\lambda \approx 0.21$ corresponds to no leading-edge singularity for both one- and two-lobed parawings. The luffing angle of

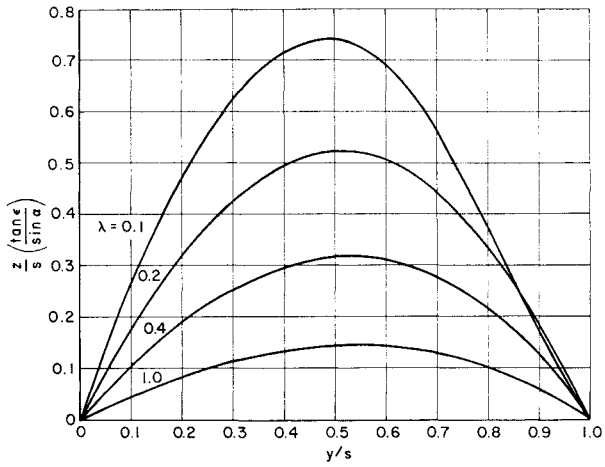

Fig. 5 Cross-sectional shapes of two-lobed conical parawings.

attack for two-lobed parawings on this basis is given as[8]

$$\sin^2\alpha_l = (\tan^2\epsilon/0.6744)[(l' - 2s)/2s] \quad (2)$$

Comparisons are made between predicted and measured trailing-edge shapes for conical, triangular parawings with one lobe and two lobes.[10] For the low-slackness range of the experimental investigation, excellent agreement was found between predicted and measured shapes.

Lifting-surface theory

Polhamus and Naeseth[14] made the assumption that the inflated canopy lobe of a two-lobed conical parawing has the same shape as part of a right-circular cone. Using this assumption, they successfully applied a combination of the Weissinger method[16] and the Pankhurst method[17] to the prediction of lift and moment of two-lobed conical parawings. More recently, the present authors, using the same approach, made an extensive investigation of two-lobed parawings, including drag predictions, shape comparisons, and leading-edge effects. The results of this latter investigation are reviewed below.

The canopy shape is specified as a portion of a right-circular cone, with the keel and leading edge lying along slant heights of the cone. From the resulting canopy-shape equation, the coordinates of any point on the canopy can be obtained. In particular, the geometric twist and section camber can be obtained.

The primary method used to obtain the canopy aerodynamic characteristics is the Weissinger method.[16] This method does not treat wing camber in a direct fashion, but can account for camber by the addition of the local angle of zero lift to the geometric twist angle. The local angles of zero lift were obtained using the Pankhurst method.[17]

The Weissinger method uses the values of wing chord at the spanwise stations at which the boundary condition is satisfied. For parawings having large twist angles at the tip, the actual chord is considerably larger than the planform chord. Use of the actual chord, rather than the planform chord, was found to help account for nonplanar wing effects, as shown by comparisons with data.

The zero-lift pitching moment determined by the Weissinger method for the equivalent uncambered, twisted wing does not include the moment due to camber. The latter moment was determined approximately by computing the section zero-lift pitching moments, pure couples, by the method of Pankhurst, and integrating these over the span to get the wing moment due to camber.

Since the Weissinger method satisfies the wing boundary condition at only one station on the chord, it cannot account for the chordwise variations of loading and induced downwash. These effects can be significant for parawings of low aspect ratio and high slackness (large camber). Consequently, an investigation was made, using the Multhopp method, which considers chordwise loading variations and satisfies the wing boundary condition at several stations along the chord. A computer program (No. A0313), developed by J. E. Lamar of the NASA Langley Research Center was used for this investigation. This program uses the method developed by van Spiegel and Wouters.[18]

Profile-drag prediction

Profile drag is generally not predictable theoretically. Consequently, section data were used in a strip-theory approach to estimate canopy profile drag. The appropriate section is a thin cambered plate. Since no section data were found for such an airfoil, the desired section characteristics

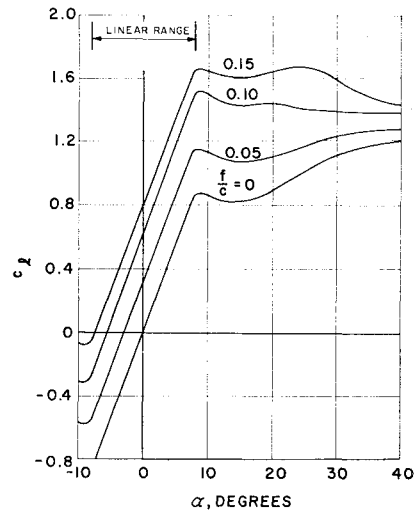

a) Lift coefficient vs angle of attack

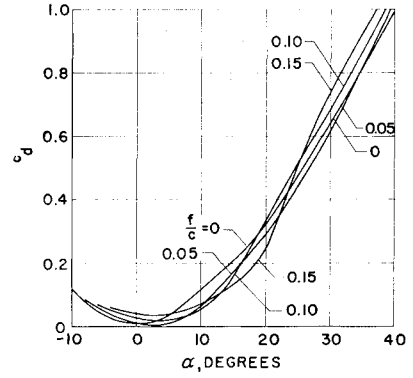

b) Drag coefficient vs angle of attack

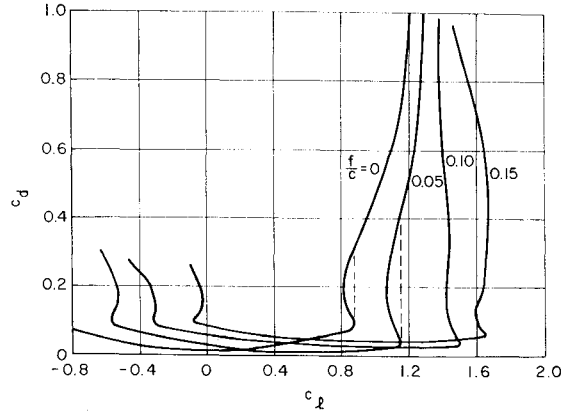

c) Drag coefficient vs lift coefficient

Fig. 6 Constructed section data for cambered plates.

were approximated by combining thin flat-plate data with camber increments deduced from aspect ratio 5, rectangular, cambered wing data.

Section lift and drag data on a flat plate were obtained from Refs. 19 and 20. The latter data were used for drag at low angles of attack because of the uncertainty of the comparable data in Ref. 19. Data for a thin, aspect ratio 5 plate with circular arc camber are available from Ref. 21. The lift coefficient increment due to camber was considered to be the difference between the lift coefficient for the cambered plate and that for the uncambered plate at a specified angle of attack. The drag coefficient increments due to camber were obtained in a similar manner; however, the drag data were corrected to infinite aspect ratio before the differences were taken. The section data used for all profile-drag calculations were obtained by adding the camber increments to the flat-plate data. The resulting set of curves is shown in Fig. 6. Linear interpolation was used for intermediate camber values.

In Fig. 6a it is interesting to note that for each camber value the section lift curve becomes nonlinear at the same angle of attack. The angle-of-attack range $-8° \leq \alpha \leq 8°$ is defined as the "linear range" of the section data. The camber and twist distributions of parawings cause large variations in local section lift coefficients across the span of the parawing, so that some sections of the wing are operating in the linear range of the section data, while others are not.

A second point of interest in the data of Fig. 6 is noteworthy. Fig. 6a indicates the experimental values of section angle of zero lift to be approximately half those predicted by the Pankhurst method. A similar comparison of c_{m_0} values indicates that the measured values are less than half those predicted by Pankhurst. It is apparent from these results that highly cambered sections do not develop their full predicted lift, probably because of viscous effects.

Several methods of applying section data to the calculation of wing profile drag were investigated. The first procedure investigated was called the "c_l method." At the local lift coefficient, c_l, given by the Weissinger method, the corresponding profile-drag coefficient c_d was found in the section data of Fig. 6c. These section-drag coefficients were then integrated over the span to get the wing profile-drag coefficient.

An interesting point arises in applying the foregoing analysis at high section-lift coefficients. With reference to Fig. 6c, near a lift coefficient of 0.85, a reversal occurs in the curve and c_d is a multivalued function of c_l. Since c_l predicted by the Weissinger method increases monotonically with α, the drag was assumed to increase discontinuously, as shown by the dashed line. Because of the many semispan stations used, the local discontinuities are small, and a continuous wing drag curve results. The c_l method thus has the characteristic that it estimates where wing stall first occurs, and how the stall region propagates as the angle of attack increases.

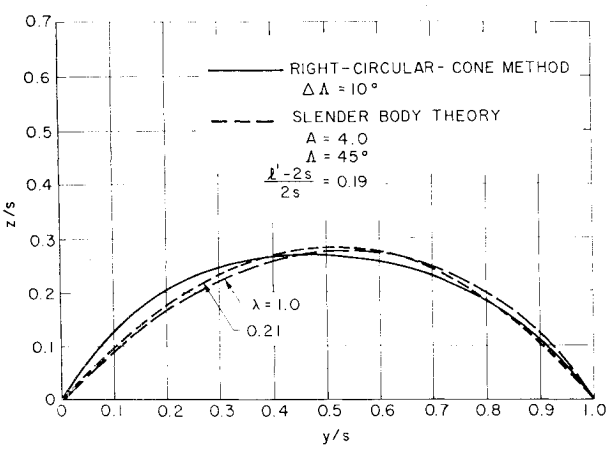

Fig. 7 Comparison of triangular wing trailing-edge shapes given by slender-body theory and the right-circular-cone method.

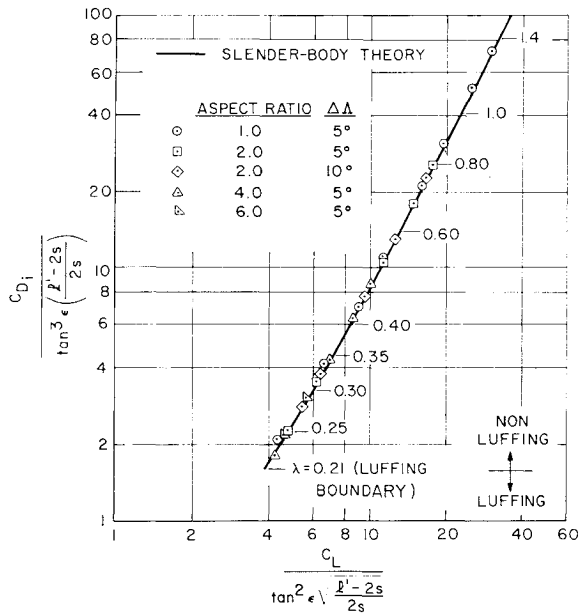

Fig. 8 Induced-drag correlation for triangular two-lobed parawings.

In the second procedure (the α-method), local section profile drag was found as a function of local section angle of attack α, where α is $\alpha_0 + c_l/2\pi$. The local angle of zero lift α_0 appears because, in the use of the Weissinger method, the effect of camber was converted to an equivalent twist. The local profile-drag coefficient was found in Fig. 6b for the actual cambered section at the appropriate angle of attack, and the total wing profile-drag coefficient was obtained by integration as before. It is noted that with this method the drag coefficient is a single-valued function of α.

No adjustments were made to the profile-drag coefficients to account for leading-edge sweep effects in either the c_l or α methods. It might be possible to develop such an adjustment, based on the work of Polhamus,[22] and the assumption that some or all leading-edge suction is lost and additional drag is incurred.

Comparison Between Theoretical Methods

Canopy shape

Two methods have been used to specify canopy shape; slender-body theory, and the right-circular-cone assumption. In order to compare these methods, slender-body trailing-edge shapes were computed for an aspect ratio 4 triangular wing for two values of tension parameters; one value at the theoretical luffing boundary ($\lambda = 0.21$), and the second at a higher lift condition ($\lambda = 1.0$). The trailing-edge shape from the right-circular-cone method was calculated for a triangular wing with the same slackness ratio. These trailing-edge shapes, compared in Fig. 7, indicate that the predicted canopy shape depends slightly on the method used. The aerodynamic characteristics of these canopies were compared on the basis of the Weissinger method. The predicted angles of zero lift and pitching moments at zero lift agree within 1 and 10%, respectively; therefore, the small difference in shape has little effect on the calculated aerodynamic characteristics.

Accuracy of lifting-surface theories

On the basis of the results of Ref. 8, the induced drag of two-lobed triangular parawings can be correlated by the di-

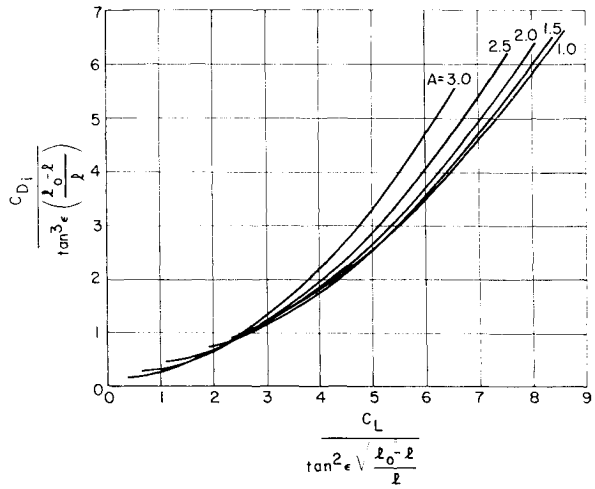

Fig. 9 Induced-drag correlation for two-lobed parawings of NASA planform.

mensionless parameters

$$\frac{C_{Di}}{\tan^3\epsilon[(l'-2s)/2s]} \text{ and } \frac{C_L}{\tan^2\epsilon[(l'-2s)/2s]^{1/2}}$$

for any aspect ratio or slackness ratio. The theoretical curve from slender-body theory is shown in Fig. 8. The induced drag calculated by the seven-point Weissinger theory for several triangular wings, whose shape is given by the right-circular-cone assumption, is shown in the same figure. It is noted that the induced drag determined on this basis is virtually the same as the induced drag from slender-body theory for wings of the same aspect ratio and slackness ratio.

Based on systematic calculations from the Weissinger method, a correlation similar to that for triangular wings is shown in Fig. 9 for NASA planforms. NASA planforms are defined as those having leading edges and keel of equal length. The results show that, for a fixed aspect ratio, all slackness ratios fall on a single curve.

Comparisons of Weissinger-Pankhurst and Multhopp predictions were made to evaluate the chordwise effects neglected in the Weissinger method. These chordwise effects consist of the chordwise variation of streamline curvature (induced camber) induced by the wing vortex system, which is most significant at low aspect ratios, and the chordwise variation of loading, which is most significant for highly cambered wings where the camber loading is concentrated near the midchord rather than at the quarter chord. The Multhopp results were obtained using 21 spanwise and six chordwise control points.

The results indicate that lift-curve slope, center of pressure, and the flat-wing portion of the induced drag are very well predicted by the Weissinger method. The differences in moment-curve slope are somewhat larger, but the agreement is considered satisfactory, except at low aspect ratio where induced-camber effects due to the trailing vortex system are important. The chordwise effects were found to have a considerable influence on angle of zero lift and moment at zero lift.

The results of the comparisons for α_0 and C_{m_0} are summarized in Fig. 10. The α_0 results of Fig. 10a indicate two effects. The first is an overprediction of α_0 by the Weissinger method at low aspect ratio because of induced camber. The second is an underprediction at high slackness due to chordwise loading, which becomes significant for $2\beta > 120°$. The results for C_{m_0} of Fig. 10b also indicate a systematic variation of the difference between the two theoretical methods. The Weissinger method consistently underpredicts C_{m_0}, with the largest differences occurring at the lower aspect ratios.

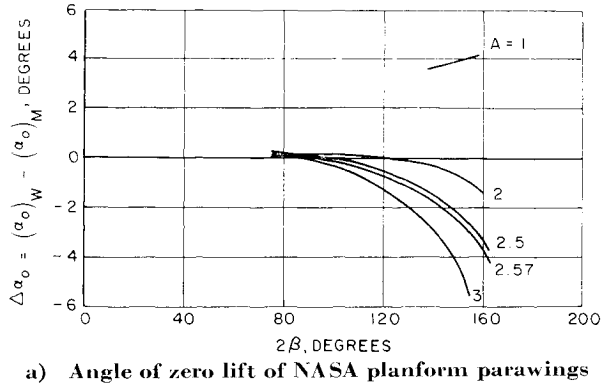

a) Angle of zero lift of NASA planform parawings

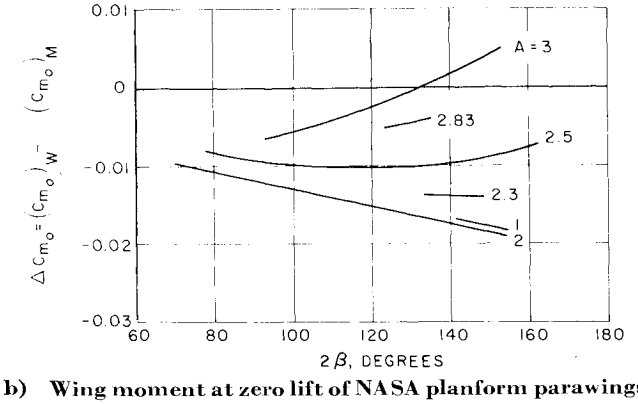

b) Wing moment at zero lift of NASA planform parawings

Fig. 10 Comparisons of Multhopp and Weissinger-Pankhurst predictions.

Comparison Between Theory and Experiment

Comparisons between the Weissinger predictions and data were made to show the accuracy of the prediction methods. The basic canopy prediction methods were checked, using data for rigid wings of known shape and no leading-edge booms. Subsequent comparisons with flexible wings were used to deduce leading-edge boom effects.

Rigid wings

Unpublished, systematic data for a series of rigid wings were made available by the NASA Langley Research Center. These wings were simulated parawings, having surfaces formed from right-circular cones. All had semicircular leading edges swept 50° and no leading-edge booms. These data were taken to represent the aerodynamic performance of the basic canopy for comparison with the Weissinger-Pankhurst method.

Comparisons between experiment and theory for wings of moderate slackness and aspect ratios 3.0 and 4.0 are shown in Fig. 11. The linear range for the wing is shown on each figure. The wing linear range is exceeded when at any spanwise station the local angle of attack calculated from the Weissinger method exceeds ±8°, since from Fig. 6a, nonlinearities appear in the lift curves of cambered circular-arc sections at ±8° angle of attack, irrespective of camber. Stall is said to occur when the local lift coefficient reaches its first maximum in Fig. 6c.

The theoretical results for α_0 and $C_{L\alpha}$ are in good agreement with the data in each case, both inside and outside the linear range. This is also true for other rigid wings of much higher slackness ratio. The good agreement of predicted gross wing lift coefficient is noteworthy, in view of the facts that the Weissinger method often predicts local lift coefficients greater than 2.0 in the regions of good agreement, that the theoretical camber increments (α_0) used in the Weissinger method are considerably higher than those shown by data, and that chordwise effects and nonplanar effects are neglected.

The induced drag computed using the Weissinger method, combined with the profile-drag results from both α and c_l methods, are shown for each wing. In the linear range, where maximum lift-drag ratio occurs, both methods yield about the same drag; however, the theoretical drag is always less than experiment. The accuracy of prediction increases as the aspect ratio and slackness ratio decrease.

An examination of the pitching-moment results of Fig. 11a indicates that good agreement was obtained on both $C_{m\alpha}$ and C_{m_0} for the aspect ratio 3 wing. Figure 11b indicates that for the aspect ratio 4 wing, the $C_{m\alpha}$ is predicted well, but the predicted C_{m_0} is high. Various sources of inaccuracy not accounted for in the Weissinger-Pankhurst prediction of C_{m_0} include nonplanar effects arising from applying the boundary condition in the plane of the leading edges, chordwise effects (Fig. 10b), pitching moment due to drag acting on the actual wing surface above the root chord plane, and the fact that highly cambered sections do not develop all of their predicted lift. Inclusion of each of the latter three effects would raise the predicted values of C_{m_0}, causing poorer agreement between experiment and theory. Thus, these effects are being compensated by either nonplanar effects or other unrecognized effects, with the net result being good agreement between the Weissinger-Pankhurst prediction and experiment. For large slackness ratios, the agreement deteriorates.

Leading-edge booms

An analytical method for predicting force and moment increments due to leading-edge booms was investigated, using strip theory and section data for a thin flat plate attached tangentially at its leading edge to the top of a circular cylinder. The method was found to be unsatisfactory in predicting the differences between the measured results for a rigid wing with no booms and the corresponding flexible wing with booms.

Leading-edge boom effects were then examined in an empirical fashion to determine if systematic increments could be found and correlated. For this purpose, differences between flexible-wing data and either rigid-wing data or the basic canopy theory (Weissinger) were assumed to be due primarily to leading-edge booms. The boom effects were found to depend on the ratio of boom diameter to canopy root chord (d/c_r), the taper of the boom, and the method of attachment of the canopy to the boom.

The angle of zero lift was found to decrease with the addition of leading-edge booms. For NASA planform parawing models with constant diameter booms ($d/c_r = 0.015$) and a pocket canopy attachment,[23] an adjustment on the Weissinger α_0 of $-2°$ was found to give good agreement with data over a wide range of slackness and aspect ratios. For NASA planform parawing models with somewhat larger constant diameter booms ($d/c_r = 0.07$) and a top attachment of the canopy,[24] an adjustment of $-4°$ was found to give good agreement. Other data examined did not indicate systematic differences.

Comparison of experimental and theoretical lift-curve slopes for a series of NASA planform wings with constant boom diameter indicated no systematic boom effects. Generally, the differences were less than 10% for $2\beta < 180°$, so that no adjustment to the Weissinger values of lift-curve slope appeared warranted. For wings with tapered leading-edge booms, however, the Weissinger values were consistently high by an amount that increased with increasing slackness.

For drag, no simple adjustments to account for leading-edge booms were found because of the more complicated influences of the leading-edge booms in this case. Almost without exception, the flexible wings showed a higher drag at low-lift coefficients and a lower drag at high-lift coefficient than the corresponding rigid wings. It is believed that the leading-edge booms tend to delay general separation at large angles of attack.

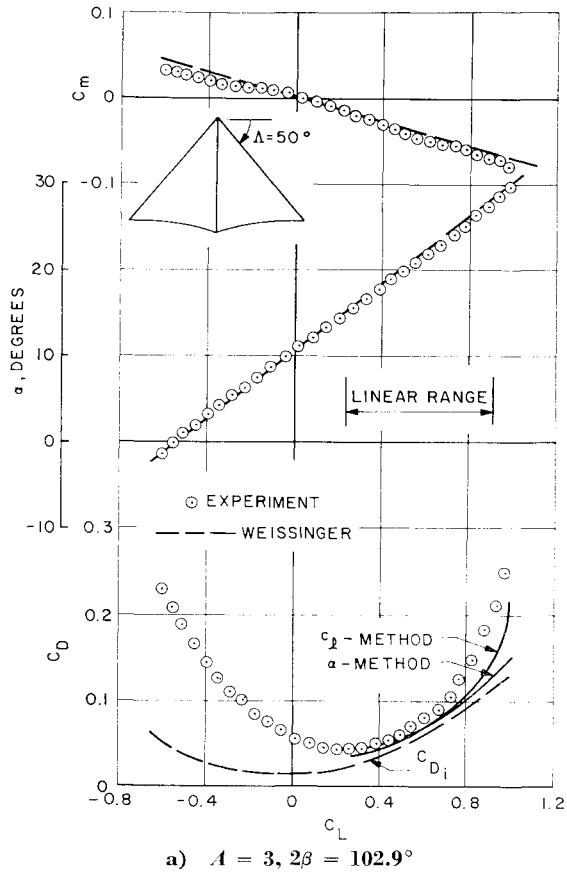

a) $A = 3$, $2\beta = 102.9°$

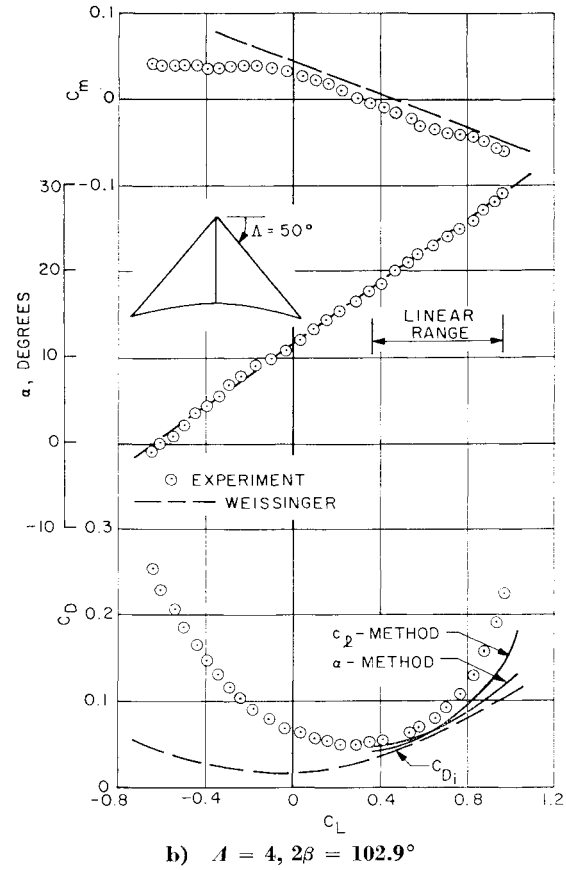

b) $A = 4$, $2\beta = 102.9°$

Fig. 11 Predicted and measured characteristics of rigid wings.

The addition of leading-edge booms causes a decrease in pitching moment for a given lift coefficient. For moderate slackness ratios, the slope dC_m/dC_L is not significantly

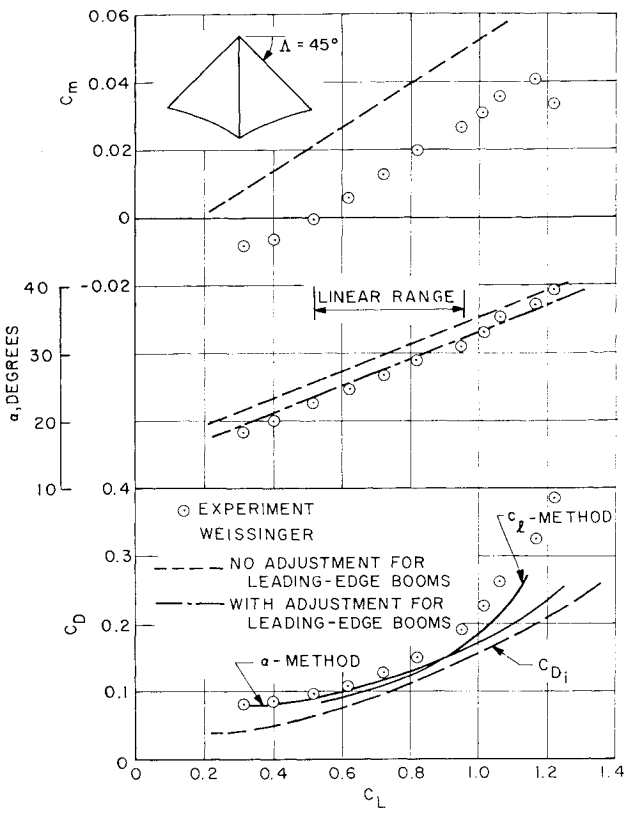

a) $A = 2.83$, $2\beta = 130.5°$

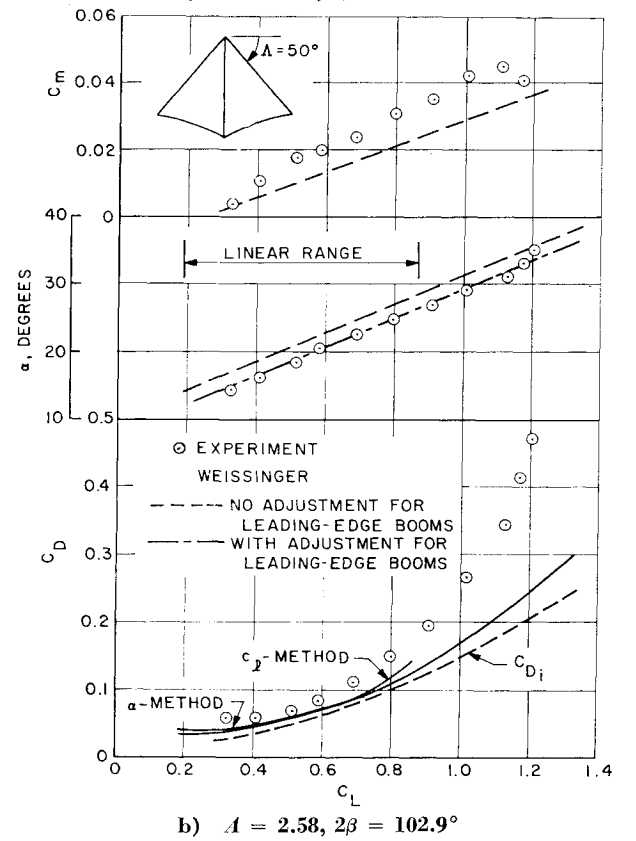

b) $A = 2.58$, $2\beta = 102.9°$

Fig. 12 Predicted and measured characteristics of flexible NASA planform parawings.

changed. Since the addition of the leading-edge booms causes positive lift and negative moment for a fixed angle of attack, the main lift is added behind the wing center of moments; however, no simple adjustment could be found to account for leading-edge boom effects on moment.

Flexible wings

The theory for the prediction of flexible-wing aerodynamic performance is not complete, since the effects of the leading-edge booms must be handled empirically. However, the previously discussed Weissinger-Pankhurst method and the canopy-shape assumption, together with empirical adjustments suggested previously, can yield reasonably good predictions in many cases, particularly in the region around maximum lift-drag ratio. Two examples are shown in Fig. 12 for NASA planform parawings with pocket attachment and $d/c_r = 0.015$. The data were taken from Ref. 23. The lift is predicted very well with the adjustment of $-2°$ for α_0 mentioned before. The drag is slightly underpredicted at moderate lift coefficients for both wings using either the c_l or the α method with no correction for leading edges. The moment slope C_{m_α} is well predicted, but the zero-lift moment is not. It is interesting to note that the theory overpredicts C_{m_0} in Fig. 12a (which is generally the case) and underpredicts C_{m_0} in Fig. 12b. These examples are typical in that lift, drag, and moment-curve slope are generally well predicted in the linear range, but C_{m_0} is not.

All-Flexible Parawings

All-flexible parawings (Fig. 2) are characterized by the absence of any rigid structure to maintain the canopy shape. A series of riser lines are attached at intervals along the two leading edges and keel that, under proper tension (i.e., proper length) maintain the canopy shape. This type of parawing is the least efficient of those discussed in this paper. Consequently, a considerable amount of work has gone into testing of different configurations,[25] including "twin-keel" versions, in which a rectangular or trapezoidal center panel is inserted to increase aspect ratio.

Very little theoretical work on the prediction of aerodynamic performance of all-flexible parawings has been done. The primary reason is the canopy shape, which is quite complex due to the interaction between the aerodynamic loads and the point-support loads from the risers. The canopy sections have very high camber (as much as 30%). Thus, planar-lifting-surface theories would not be expected, a priori, to give satisfactory results for aerodynamic loading. An additional problem with the canopy shape is the creases formed where the risers remove the load from the canopy. The viscous effects caused by the large camber and the creases may have a significant effect on the canopy loading.

Another problem peculiar to the all-flexible parawing is the relation between the riser line length, riser tension, canopy shape, and aerodynamic loading. Change in length of one of the riser lines will result in a change in canopy shape, loading, and the tensions in the other risers. Thus, the suspension system (line placement and length) must play an intimate role in the aerodynamic prediction method. Also, it is probable that very little leading-edge suction can be developed by all-flexible parawings, so that they must be designed to produce lift principally by camber. A rational theory for such wings remains to be developed.

Concluding Remarks

This paper has reviewed analytical methods for predicting the characteristics of various types of parawings. Most analytical work has been directed toward two-lobed conical parawings with relatively small leading-edge booms, since this configuration has been most extensively investigated for practical applications to date. There has been great interest more recently in the all-flexible parawing, because of its advantages in compact stowage and simpler deployment.

For two-lobed conical parawings, the prediction methods for the longitudinal aerodynamic characteristics are in a comparatively good state. Additional work can profitably be undertaken on the prediction of profile drag, including

obtaining better section data. Additional work is desirable on leading-edge effects, which should include additional systematic tests and correlation on boom size, boom taper, and boom attachment means for potentially efficient boom configurations.

The need for theoretical work exists for the all-flexible parawing, because of present interest in this configuration, and because no theoretical basis exists to understand its behavior. Any analytical approach will probably have to include consideration of the rigging constraints.

References

[1] Rogallo, F. M., "Introduction to Aeroflexibility," presented April 21, 1954 to ARDC Unit at Langley Field, Va.

[2] Gamse, B., Mort, K. W., and Yaggy, P. F., "Low-Speed Wind-Tunnel Tests of a Large-Scale Inflatable Structure Paraglider," TN D-2849, June 1965, NASA.

[3] "Flexible-Wing Precision Drop Glider," Final Rept. AD 426250, Dec. 1963, Ryan Aeronautical Co.

[4] Voelz, K., "Profil und Auftrieb eines Segels," *Zeitschrift fuer Angewandte Mathematik und Mechanik,* Band 30, Heft 10, Oct. 1950.

[5] Thwaites, B., "The Aerodynamic Theory of Sails. I. Two-Dimensional Sails," *Proceedings of the Royal Society,* Ser. A, Vol. 261, 1961, pp. 402–422.

[6] Nielsen, J. N., "Theory of Flexible Aerodynamic Surfaces," *Journal of Applied Mechanics,* Vol. 30, Ser. E, No. 3, Sept. 1963, pp. 435–442.

[7] Nielsen, J. N., Kriebel, A. R., and Goodwin, F. K., "Theoretical Aerodynamics of One-Lobed Flexible Parawings at Low Speeds," *Journal of Aircraft,* Vol. 2, No. 2, March-April 1965, pp. 127–135.

[8] Nielsen, J. N. et al., "Theoretical Aerodynamics of Flexible Wings at Low Speeds. II. Two-Lobed Parawings," Rept. 133, AD 601-848, May 1964, Vidya Div., Itek Corp.

[9] Kriebel, A. R. and Nielsen, J. N., "Theoretical Aerodynamics of Flexible Wings at Low Speeds. III. Approximate Results for Wings of Large Aspect Ratio," Rept. 146, AD 606-059, July 1, 1964, Vidya Div., Itek Corp.

[10] Burnell, J. A. and Nielsen, J. N., "Theoretical Aerodynamics of Flexible Wings at Low Speeds. IV. Experimental Program and Comparison with Theory," Rept. 172, Feb. 16, 1965, AD 617-925, Vidya Div., Itek Corp.

[11] Nielsen, J. N. and Burnell, J. A., "Theoretical Aerodynamics of Flexible Wings at Low Speeds. V. Engineering Method for Estimating Parawing Performance," Rept. 209, AD 628-579, Dec. 1, 1965, Vidya Div., Itek Corp.

[12] Nielsen, J. N., Lynes, L. L., and Goodwin, F. K., "The Theoretical Characteristics of One-Lobed Parawings in Combined Pitch and Sideslip," Rept. 220, May 1966, Vidya Div., Itek Corp.

[13] Gersten, K. and Hucho, W. H., "Theoretische und Experimentalle Untersuchungen an Flexiblen Flügeln," Bericht Nr. 65/27, 1965, Institut für Strömungsmechanik.

[14] Polhamus, E. C. and Naeseth, R. L., "Experimental and Theoretical Studies of the Effects of Camber and Twist on the Aerodynamic Characteristics of Parawings Having Nominal Aspect Ratios of 3 and 6," TN D-972, Jan. 1963, NASA.

[15] Fralich, R. W., "Stress and Shape Analysis of a Paraglider Wing," *Journal of Applied Mechanics,* Vol. 32, No. 4, Dec. 1965, pp. 771–780.

[16] DeYoung, J. and Harper, C. W., "Theoretical Symmetric Span Loading at Subsonic Speeds for Wings Having Arbitrary Planform," Rept. 921, 1948, NACA.

[17] Pankhurst, R. C., "A Method for the Rapid Evaluation of Glauert's Expressions for the Angle of Zero Lift and the Moment at Zero Lift," R&M 1914, March 23, 1944, Aeronautical Research Council.

[18] van Spiegel, E. and Wouters, J. G., "Modifications of Multhopp's Lifting Surface Theory with a View to Automatic Computation," Rept. NLR-TN W.2, June 1962 National Aero- and Astronautical Research Institute, Amsterdam.

[19] Wick, B. H., "Study of the Subsonic Forces and Moments on an Inclined Plate of Infinite Span," TN 3221, June 1954, NACA.

[20] Lindsey, W. F. and Landrum, E. J., "Flow and Force Characteristics of 2-Percent-Thick Airfoils at Transonic Speeds," RM L54I30, Jan. 1955, NACA.

[21] Flachsbart, O., "Messungen an ebenen and gewölbten Platen," *Ergebnisse der Aerodynamischen Versuchsanstalt zu Gottingen,* edited by L. Prandtl and A. Betz, Oldenbourg, Munich and Berlin, Vol. II, 1932, pp. 96–100.

[22] Polhamus, E. C., "A Note on the Drag Due to Lift of Rectangular Wings of Low Aspect Ratios," TN 3324, Jan. 1955, NACA.

[23] Naeseth, R. L. and Gainer, T. G., "Low-Speed Investigation of the Effects of Wing Sweep on the Aerodynamic Characteristics of Parawings Having Equal-Length Leading Edges and Keel," TN D-1957, Aug. 1963, NASA.

[24] Croom, D. R., Naeseth, R. L., and Sleeman, W. C., "Effects of Canopy Shape on Low-Speed Aerodynamic Characteristics of a 55° Swept Parawing with Large Diameter Leading Edges," TN D-2551, Dec. 1964, NASA.

[25] Naeseth, R. L. and Fournier, P. G., "Low-Speed Wind-Tunnel Investigation of Tension-Structure Parawings," TN D-3940, June 1967, NASA.